

of **3** (5:1 ratio) in 0.6 mL of C_6D_6 (94 h, 140 °C, sealed tube) results in the formation of 7-methylindole in 70% isolated yield after sublimation (3.5 turnovers).

The mechanism of this cyclization was revealed in reactions under less severe conditions. Thermolysis of **3** in C_6D_6 under 534 mm of D_2 at 140 °C results in the slow formation of **3-d₂** (84% exchange after 33 h). Irradiation of **3** for 2 h in the presence of 2,6-xylyl isocyanide at 25 °C produces ~25% yield of a new product formulated as $Ru(DMPE)_2(CN-2,6-C_6H_3Me_2)$ (**4**), on the basis of the similarity of the 1H NMR spectral data to that of other $Ru(DMPE)_2L$ ($L = CNPh, CNCH_2CMe_3, CO, PMe_3$) complexes.^{7,8} Upon standing at 25 °C, a C_6D_6 solution of **4** produces *trans*-**2** quantitatively (by 1H NMR) after several days. Furthermore, heating a benzene solution of *trans*-**2** in a sealed tube under 540 mm of H_2 to 100 °C induces isomerization to *cis*-**2**.⁹ Raising the temperature to 140 °C results in the rapid production of free 7-methylindole and **3** (95% complete in 2 h).

A proposed mechanism for this reaction is shown in Scheme I involving coordination of isocyanide to $[Ru(DMPE)_2]$ and dissociation of one end of a DMPE ligand followed by benzylic methyl group oxidative addition to generate a six-membered metallocycle ring.¹⁰ The isocyanide insertion into the $Ru-CH_2$ bond is driven by the closure of the DMPE chelate to give stereospecifically the *trans* isomer. Tautomerism of the methylene hydrogen to the nitrogen generates the observed product *trans*-**2**. Isomerization from *trans* to *cis* occurs prior to reductive elimination, with the latter being the highest barrier in the catalytic cycle.

Several novel conclusions arise as a consequence of the proposed mechanism. First, while the intermediate in which the $C-H$ bond undergoes oxidative addition to the metal might appear to be rather strained due to the anticipated linearity of the $Ru-C-N-C$ linkage, the intramolecular oxidative addition still occurs. A resonance structure involving strong π -back-bonding with the $Ru(0)$ center would manifest itself in both the reduction of the isocyanide stretching frequency and bending of the $C-N-C$ bond. Another interesting feature of this system is that *C-H activation occurs even in the presence of an excess of the trapping ligand* (CNR), the reaction occurring due to the formation of a second vacant coordination site on ruthenium. Finally, this new route to indoles (most similar to the Madelung synthesis^{11a} or the

lithiation procedure of Ito and Saegusa^{11b}) offers advantages over the traditional routes in that neutral conditions and lower temperatures are employed.^{11c} Further extensions of this cyclization to include other indoles and heterocycles are under investigation.

Acknowledgement is made to the U. S. Department of Energy (DE-AC02-83ER13095) for their partial support of this work. W. D. J. also thanks the Alfred P. Sloan and Camille and Henry Dreyfus Foundations for Awards.

Supplementary Material Available: Description of the structural solution and an ORTEP plot of *trans*-**2**, tables of crystallographic data collection parameters, fractional atomic coordinates, anisotropic thermal parameters, and bond distances and angles (7 pages); table of calculated and observed structure factors (20 pages). Ordering information is given on any current masthead page.

The Sonochemical Hot Spot

Kenneth S. Suslick,* David A. Hammerton, and Raymond E. Cline, Jr.

School of Chemical Sciences
University of Illinois at Urbana—Champaign
Urbana, Illinois 61801
Received April 7, 1986

The chemical effects of ultrasound have been studied for over 50 years.^{1,2} In spite of this, our understanding of the reaction conditions created by ultrasonic irradiation of liquids is extremely limited. It is well accepted^{2,3} that sonochemistry results from acoustic cavitation: the creation, expansion, and implosive collapse of bubbles in ultrasonically irradiated liquids.⁴ We have used the sonochemical ligand substitution rates of volatile metal carbonyls to establish the site of sonochemical reactions.⁵ We find that there are two regions of sonochemical reactivity: one corresponding to the gas phase within the collapsing cavity and the second to a thin liquid layer immediately surrounding the collapsing cavity. Furthermore, we are now able to determine experimentally the effective temperature in each reaction zone, through the use of comparative rate thermometry. The gas- and liquid-phase reaction zones have effective temperatures of 5200 and 1900 K, respectively.

In order to probe the nature of the sonochemical hot spot, we wished to determine the first-order rate coefficients of sonochemical ligand substitution as a function of metal carbonyl vapor pressure. However, the efficacy of cavitation collapse and the temperatures so generated are strongly dependent on the vapor pressure of the solvent system.⁶ Therefore, sonolyses at various ambient temperatures were done in solutions of two *n*-alkanes which had been mixed in the proper proportion to keep the total system vapor pressure constant (at 5.0 torr).⁷ Alkane solutions of metal carbonyls (0.01 M) were irradiated with a collimated

(6) 7-methylindole and 2,6-xylyl isocyanide do not react at 140 °C in the absence of **3**. In the presence of **3**, the amount of dimer increases (up to 35% of the reaction mixture) and then decreases as isocyanide is converted into indole. 1H NMR of dimer (C_6D_6): δ 8.550 (s, 1 H), 8.369 (d, $J = 3.6$ Hz, 1 H), 7.387 (d, $J = 7.8$ Hz, 1 H), 7.00 (m, 4 H), 6.817 (d, $J = 7.2$ Hz, 1 H), 6.510 (d, $J = 4.1$ Hz, 1 H), 2.152 (s, 6 H), 1.966 (s, 3 H). ^{13}C NMR ($CDCl_3$, attached proton test polarization shown in parentheses where observed): δ 18.61 (-), 21.81 (-), 108.28 (-), 119.83 (-), 121.18 (+), 122.14 (-), 123.75 (-), 123.93 (-), 127.15 (-), 128.29 (-), 128.66 (+), 131.34 (+), 134.34 (n.o.), 145.62 (-), 147.79 (n.o.). IR (C_6H_6): 1647 cm^{-1} . Mass spectrum (75 eV): 262 (M^+), 131, 130.

(7) (a) Jones, W. D.; Libertini, E. *Inorg. Chem.* **1986**, *25*, 1794-1800. (b) Jones, W. D.; Kosar, W. P. *Organometallics*, in press.

(8) 1H NMR of **4** in C_6D_6 : δ 6.993 (d, $J = 7.4$ Hz, 2 H); 6.856 (t, $J = 7.5$ Hz, 1 H); 2.672 (s, 6 H); 1.300 (br s, 24 H). IR (KBr): $\nu_{C-N} = 2048$ cm^{-1} .

(9) 1H NMR of *cis*-**2** in C_6D_6 : δ 8.074 (br s, 1 H); 7.204 (t, $J = 7.4$ Hz, 1 H); 6.908 (d, $J = 7.1$ Hz, 1 H); 7.686 (d, $J = 7.6$ Hz, 1 H); 6.314 (s, 1 H); 2.491 (s, 3 H); 1.427 (d, $J = 6.1$ Hz, 3 H); 1.210 (d, $J = 7.2$ Hz, 3 H); 1.124 (d, $J = 6.4$ Hz, 3 H); 1.059 (d, $J = 6.0$ Hz, 3 H); 0.960 (d, $J = 8.7$ Hz, 3 H); 0.934 (d, $J = 9.1$ Hz, 3 H); 0.895 (d, $J = 5.3$ Hz, 3 H); 0.852 (d, $J = 5.6$ Hz, 3 H); 0.8-1.5 (m, ~8 H (broad resonance under DMPE doublets); -8.955 (dq, $J = 83.6, 24.4$ Hz, 1 H).

(10) $Ru(\eta^2-DMPE)(\eta^1-DMPE)(CNPh)_2$ forms from the reaction of $Ru(\eta^2-DMPE)_2(CNPh)$ with $CNPh$. See ref 7b.

(11) (a) Sundberg, R. J. *The Chemistry of Indoles*; Academic Press: New York, 1970; pp 189-191. (b) Ito, Y.; Kobayashi, K.; Seko, N.; Saegusa, T. *Bull. Chem. Soc. Jpn.* **1984**, *57*, 73-84. (c) *The Chemistry of Heterocyclic Compounds. Indoles, Part I*; Brown, R. K., Ed.; Wiley-Interscience: New York, 1972; pp 227-558.

* Author to whom correspondence should be addressed.

(1) Elpiner, I. E. *Ultrasound: Physical, Chemical, and Biological Effects*; Consultants Bureau: New York, 1964.

(2) (a) Suslick, K. S. *Adv. Organomet. Chem.* **1986**, *25*, 73-119. (b) Suslick, K. S. *Modern Synthetic Methods*; Springer-Verlag: New York, 1986; Vol. 4, pp 1-60. (c) Suslick, K. S., Ed. *Ultrasound: Its Chemical, Physical and Biological Effects*; VCH Publishers: New York, 1986.

(3) (a) Fitzgerald, M. E.; Griffing, V.; and Sullivan, J. J. *Chem. Phys.* **1956**, *25*, 926. (b) Margulis, M. A. *Russ. J. Phys. Chem. (Engl. Transl.)* **1981**, *55*, 81. (c) Sehgal, C. M.; Verrall, R. E. *Ultrasonics* **1982**, *20*, 37.

(4) Apfel, R. E. *Methods Exp. Phys.* **1981**, *19*, 355.

(5) (a) Suslick, K. S.; Hammerton, D. A. *IEEE Trans. Sonics Ultrason.* **1986**, *SU-33*, 143. (b) Suslick, K. S.; Hammerton, D. A. *Ultrasonics Intl.* **1985**, 231. (c) Suslick, K. S.; Cline, R. E., Jr.; Hammerton, D. A. *Ultrason. Symp. Proc.* **1985**, 2, 1116.

(6) (a) Suslick, K. S.; Gawienowski, J. W.; Schubert, P. F.; Wang, H. H. *J. Phys. Chem.* **1983**, *87*, 2299. (b) Suslick, K. S.; Gawienowski, J. W.; Schubert, P. F.; Wang, H. H. *Ultrasonics* **1984**, *22*, 33.

(7) (a) All vapor pressures were calculated from available data assuming ideal behavior. (b) Riddick, J. A.; Bunger, W. G. *Tech. Org. Chem. (N.Y.)* **1970**, 2. (c) Dilbert, A. G.; Sulzmann, K. G. P. *J. Electrochem. Soc.* **1974**, *121*, 832. (d) Fabbri, L.; Mascherini, R.; Paoletti, P. *J. Chem. Soc., Faraday Trans. 1* **1976**, *72*, 896.

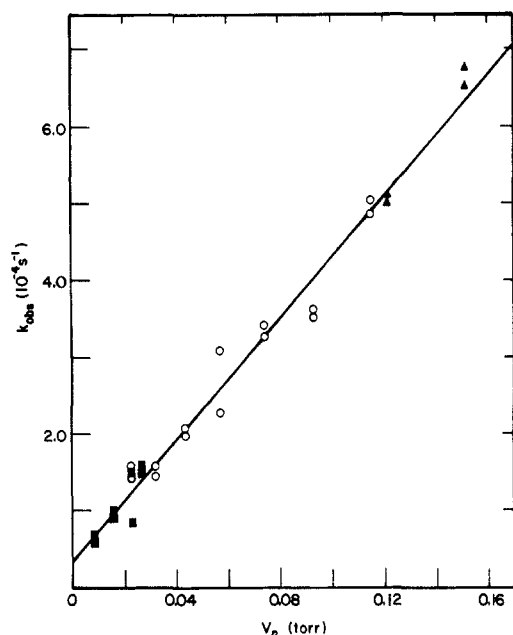


Figure 1. Observed first-order rate constants for the sonolysis of $\text{Fe}(\text{CO})_5$ vs. the vapor pressure of $\text{Fe}(\text{CO})_5$. Total vapor pressure of the solvent system is constant at 5.0 torr. The gas-phase reaction coefficient, k_g , is determined from the slope, the liquid-phase coefficient, k_l , from the intercept. For each of the following substrates, k_g (in $\text{s}^{-1} \text{bar}^{-1}$) and k_l (in $\text{s}^{-1} \text{M}^{-1}$) are listed with the standard deviation of the last digit in parentheses: $\text{Fe}(\text{CO})_5$, 2.96 (5), $3.35 (48) \times 10^{-3}$; $\text{Cr}(\text{CO})_6$, 2.45 (72), $12.2 (10) \times 10^{-3}$; $\text{Mo}(\text{CO})_6$, 1.63 (14), $2.97 (25) \times 10^{-3}$; $\text{W}(\text{CO})_6$, 1.17 (6), $1.37 (18) \times 10^{-3}$.

beam of ultrasound at 20 kHz, in the presence of excess triphenylphosphine, as described in detail elsewhere.⁸ In this fashion, the first-order rate coefficients were determined as a function of metal carbonyl vapor pressure, for $\text{Fe}(\text{CO})_5$, $\text{Cr}(\text{CO})_6$, $\text{Mo}(\text{CO})_6$, and $\text{W}(\text{CO})_6$.

In all cases the observed sonochemical rate coefficient increases linearly with increasing metal carbonyl vapor pressure and has a nonzero intercept; an example is shown in Figure 1. The linear dependence of the observed rate coefficients on metal carbonyl vapor pressure is expected for reactions occurring in the gas phase: as the substrate's vapor pressure increases, its concentration within the gas-phase cavity increases linearly, thus increasing the observed sonochemical rate coefficients. In addition, the nonzero intercept indicates that there is also a vapor pressure independent (i.e. liquid phase) component of the overall rate.

We can further analyze our data to estimate the effective temperatures reached in each site by the use of comparative rate thermometry, a technique developed for similar use in shock tube chemistry.⁹ The gas- and liquid-phase rate coefficients (k_g and k_l) are determined as shown in Figure 1. The average effective temperature of each site can then be calculated from the Arrhenius expression, using the activation parameters recently determined by high-temperature gas-phase laser pyrolysis.¹⁰ We find that the gas-phase reaction zone effective temperature is 5200 ± 650 K, and the liquid-phase effective temperature is ≈ 1900 K.

For comparison, theoretical calculations using hydrodynamic models of cavitation collapse have given temperature and pressure estimates of 2000–10000 K and 1000–10000 bar.¹¹ Prior

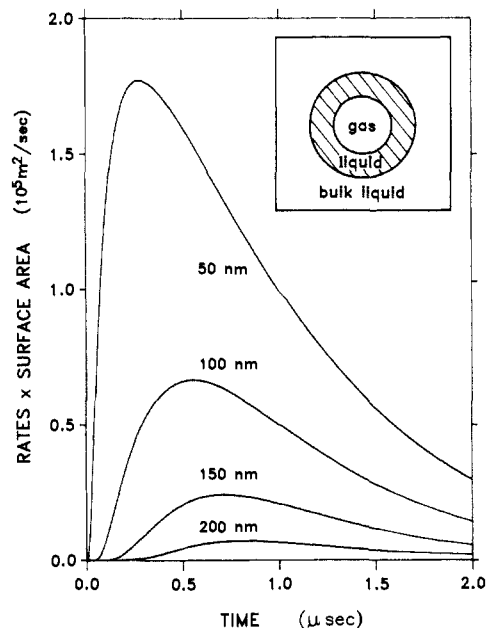


Figure 2. Temporal and spatial evolution of reaction rates in the liquid-phase reaction zone. Rates were calculated as a function of time and distance from the bubble surface assuming only conductive heat transport from a sphere with radius $150 \mu\text{m}$ at 5200 K , embedded in an infinite matrix at 300 K . The inset represents the proposed two-site model, but it is not to scale!

experimental evidence on the conditions generated during cavitation collapse is sparse and is based exclusively on sonoluminescence in aqueous solutions¹² which may or may not directly probe the cavitation site.

During the cavitation collapse, the local temperature will be a time-dependent spatial gradient in the liquid surrounding the gas-phase hot spot. A more realistic view is shown in Figure 2. We have calculated the temporal and spatial evolution of the liquid-zone temperature with a heat transport model calculated by an explicit method of finite differencing.¹³ This simple model includes only conductive heat transport from a sphere; there are no adjustable parameters in predicting relative rates. The qualitative comparison is excellent. The model predicts relative liquid-phase rates to be in the same order actually observed: $\text{Cr}(\text{CO})_6 > \text{Fe}(\text{CO})_5 > \text{Mo}(\text{CO})_6 > \text{W}(\text{CO})_6$, which is different from that observed for the gas-phase site. The quantitative comparisons are fair. The model predicts a spatial and temporal average liquid-zone reaction temperature of 2730 K , while the experimentally determined data give a liquid-zone temperature of $\approx 1900 \text{ K}$. Convection and mass transport effects, which have been neglected, would lower the predicted effective temperature and improve the quantitative agreement with the observed data.

The conduction model also gives us a sense of scale concerning the liquid reaction zone. It extends only $\approx 200 \text{ nm}$ from the bubble surface and has an effective lifetime of less than $2 \mu\text{s}$ after collapse. The size of the heated shell corresponds to a reactive liquid layer of ≈ 500 molecules thick. Another way to estimate the depth of this liquid zone is to assume complete reaction of all metal carbonyl molecules in both the gas-phase and liquid-phase zones. We calculate⁵ the radius of the bubble after collapse to be $\approx 150 \mu\text{m}$; the depth of the liquid-phase reaction zone is then estimated to be $\approx 270 \text{ nm}$, in good agreement with our simple conduction model.

Acknowledgment. We thank the National Science Foundation (CHE 8319929) for its generous support. K.S.S. gratefully acknowledges an N.I.H. Research Career Development Award and a Sloan Foundation Research Fellowship.

(8) (a) Suslick, K. S.; Schubert, P. F.; Goodale, J. W. *Ultrason. Symp. Proc.* **1981**, 2, 612. (b) Suslick, K. S.; Goodale, J. W.; Wang, H. H.; Schubert, P. F. *J. Am. Chem. Soc.* **1983**, *105*, 5781. (c) Suslick, K. S.; Schubert, P. F. *J. Am. Chem. Soc.* **1983**, *105*, 6042. (d) Suslick, K. S.; Johnson, R. E. *J. Amer. Chem. Soc.* **1984**, *106*, 6856.

(9) Tsang, W. In *Shock Waves in Chemistry*; Lifshitz, A., Ed.; Marcel Dekker: New York, 1981; p 59.

(10) Lewis, N. F.; Golden, D. M.; Smith, G. P. *J. Am. Chem. Soc.* **1984**, *106*, 3905.

(11) (a) Rayleigh, Lord. *Phil. Mag.* **1917**, *34* (Ser. 6), 94. (b) Margulis, M. A.; Dmitrieva, A. F. *Zh. Fiz. Khim.* **1982**, *56*, 323. (c) Fujikawa, S.; Akamatsu, T. *J. Fluid. Mech.* **1980**, *97*, 481.

(12) (a) Sehgal, C. M.; Steer, R. P.; Sutherland, R. G.; Verrall, R. E. *J. Chem. Phys.* **1979**, *70*, 2242. (b) Sehgal, C. M.; Sutherland, R. G.; Verrall, R. E. *J. Phys. Chem.* **1980**, *84*, 396. (c) Chendke, P. K.; Fogler, H. S. *J. Phys. Chem.* **1985**, *89*, 1673.

(13) Özisik, M. N. *Basic Heat Transfer*; McGraw-Hill: New York, 1977.